

## Study of the $B^0 \rightarrow K^* \mu^+ \mu^-$ decay channel

---

**Marcella Bona**

*Queen Mary, University of London*

*E-mail:* [m.bona@qmul.ac.uk](mailto:m.bona@qmul.ac.uk)

**Mauro Dinardo**

*Università degli Studi di Milano Bicocca and INFN*

*E-mail:* [mauro.dinardo@unimib.it](mailto:mauro.dinardo@unimib.it)

**Nicola Serra**

*University of Zurich*

*E-mail:* [nicola.serra@cern.ch](mailto:nicola.serra@cern.ch)

Studies of the  $B^0 \rightarrow K^{*0} \mu^+ \mu^-$  decay are reported here comparing strategies and selections adopted by the three LHC experiments ATLAS, CMS and LHCb. Results for the angular distributions and differential branching fraction are reported and compared using the full 2011 datasets from the three collaborations. The results are consistent with the Standard Model predictions. Prospects for the future developments of these analyses are also given.

*VI Italian workshop on p-p physics at the LHC,*

*8-10 May 2013*

*Acquario di Genova, Ponte Spinola, Area Porto Antico, Genova, Italy*

## 1. Introduction

The decay  $B^0 \rightarrow K^* \mu^+ \mu^-$  is a flavour changing neutral current process that proceeds via electroweak box or penguin diagrams in the Standard Model (SM). Beyond the SM, new particles can enter in loop-order diagrams with comparable amplitudes and lead to deviations from SM predictions. This decay has been vastly studied in literature, from both the theory (see for instance [1, 2, 3, 4] and references therein) and the experimental [5, 6, 7, 8] points of view. In this decay there are several angular observables that are strongly sensitive to new physics contributions in a variety of models. The decay is completely described by the three angles  $\theta_l$ ,  $\theta_K$  and  $\phi$  and the di-muon invariant mass squared  $q^2$ . The angle  $\theta_l$  is between the  $\mu^+$  and the  $\bar{B}^0$  in the di-muon rest frame; the angle  $\theta_K$  is between the kaon and the  $\bar{B}^0$  in the  $\bar{K}^*$  rest frame; the angle  $\phi$  is between the decay planes of the di-muon pair and the  $\bar{K}^*$ , in the  $\bar{B}^0$  rest frame. After neglecting lepton mass terms and possible scalar contributions the probability density function (pdf) that describes the angular distribution of the decay products in each  $q^2$  bin is [2]:

$$\begin{aligned} \frac{1}{\Gamma} \frac{d^3(\Gamma + \bar{\Gamma})}{d \cos \theta_l d \cos \theta_K d \phi} = & \frac{9}{32\pi} \left[ \frac{3}{4} (1 - F_L) \sin^2 \theta_K + F_L \cos^2 \theta_K + \frac{1}{4} (1 - F_L) \sin^2 \theta_K \cos 2\theta_l \right. \\ & - F_L \cos^2 \theta_K \cos 2\theta_l + \frac{1}{2} (1 - F_L) A_T^{(2)} \sin^2 \theta_K \sin^2 \theta_l \cos 2\phi + \\ & S_4 \sin 2\theta_K \sin 2\theta_l \cos \phi + S_5 \sin 2\theta_K \sin \theta_l \cos \phi + \frac{4}{3} A_{FB} \sin^2 \theta_K \cos \theta_l + \\ & \left. S_7 \sin 2\theta_K \sin \theta_l \sin \phi + S_8 \sin 2\theta_K \sin 2\theta_l \sin \phi + S_9 \sin^2 \theta_K \sin^2 \theta_l \sin 2\phi \right], \end{aligned} \quad (1.1)$$

where the observables are bilinear combinations of the  $K^*$  decay amplitudes that vary with  $q^2$  and should be interpreted as average between  $B^0$  and  $\bar{B}^0$ . However in some cases, for instance  $S_7$ ,  $S_8$ , and  $S_9$ , the CP-average observables are suppressed by the small strong phases, therefore for these observables the corresponding CP asymmetries  $A_7$ ,  $A_8$ , and  $A_9$  give a better sensitivity to new physics. In addition, in the case of S-wave pollution due to the non-resonant  $B^0 \rightarrow K^+ \pi^- \mu^+ \mu^-$  decay or to higher scalar  $K^*$  resonances (for instance  $K^{*0}(1430)$ ), more terms are added to the angular distribution. These are the S-wave fraction  $F_s$  and the interference terms of the S-wave amplitude with the  $K^*$  transversity amplitudes (see [9] and references therein). In particular,  $A_s$  is a forward-backward asymmetry with respect to the angle  $\theta_K$ , generated by the interference between the S-wave and the  $K^*$  longitudinal polarisation. Finally, the  $q^2$  point where the  $A_{FB}$  changes sign (zero-crossing point) is well predicted by theory and sensitive to physics beyond the SM. In this document, the measurements recently performed by the three LHC experiments ATLAS, CMS and LHCb of this decay are discussed.

## 2. Analysis selections and strategies

The analyses reported here have been performed by the three LHC collaborations and detailed in the following references: [10] for ATLAS, [11] for CMS and [12] for LHCb. The three detectors and their performances are found here: [13] for ATLAS, [14] for CMS and [15] for LHCb. Amongst the detector characteristics, the most relevant to the study of this channel is the particle identification that allows LHCb to separate  $K/\pi$  in a momentum range of 2 – 100 GeV/c.

The studies described here used the full datasets collected in 2011 by the three LHC collaborations: 4.9, 5.2, and 1.0 fb<sup>-1</sup> of data for ATLAS, CMS and LHCb, respectively. Crucial ingredient in the data collection is the trigger. ATLAS and CMS rely on contributions from several triggers with muon  $p_T$  thresholds in the range [3 – 6] GeV/c. CMS in addition requires good di-muon vertex quality, di-muon invariant mass  $m_{\mu\mu}$  in the range  $1 < m_{\mu\mu} < 4.8$  GeV/c<sup>2</sup> and a significant separation between the beam-spot (BS) and the di-muon vertex in the transverse plane, LHCb triggers on at least one muon with  $p_T > 1.5$  GeV/c, at least one hadron with  $p_T > 1.5$  GeV/c, a large impact parameter with respect to the primary vertex (PV) and on the kinematic properties of the  $B^0$  candidates.

The  $B$  candidate selection for the three experiments is based on a significantly good separation between the  $B^0$  vertex and the primary vertex (or the BS for CMS) and on a small angle between the  $B^0$  momentum and its line of flight from the PV (or the BS for CMS). To select the  $K\pi$  pair, ATLAS and CMS rely on the track combination with the invariant mass closer to the value of the  $K^{*0}$  mass, while LHCb includes the  $K/\pi$  separation information in the multivariate classifier used in the final selection. The resonances  $J/\psi$  and  $\psi(2S)$  are vetoed by excluding di-muon mass regions around the peaks. The widths of these regions are chosen according to the mass resolutions and to take into account the radiative tails of the charmonium decays.

Given the still limited statistics, for ATLAS and CMS the peaking backgrounds other than  $K^{*0}J/\psi$  and  $K^{*0}\psi'$  are found to be negligible. LHCb performs a thorough study of several sources of peaking backgrounds: backgrounds that are not reduced to a negligible level by the selection<sup>1</sup> are explicitly vetoed or included in the systematic uncertainties. To discriminate against the combinatorial background, LHCb uses a Boosted Decision Tree (BDT), exploiting information about the event kinematics, vertex and track quality, impact parameter and particle identification information from the RICH and muon detectors. It is trained using 36 pb<sup>-1</sup> of 2010 data.

The angular and differential branching fraction analyses are performed in six bins of  $q^2$  defined as in Ref.[6]. The results on the differential branching fraction  $d\mathcal{B}/dq^2$ , on the longitudinal polarisation fraction  $F_L$  and the scalar fraction  $F_S$  are extracted from unbinned extended maximum likelihood fits to the  $B^0$  invariant mass and the angular variables. ATLAS performs a sequential fit procedure, where in a first step the invariant  $K\pi\mu\mu$  mass distribution is fitted; the resulting parameters are fixed and in a second step the angular distributions of  $\theta_K$  and  $\theta_\ell$  are fitted to obtain  $F_L$  and  $A_{FB}$ . CMS performs a first fit to the data to the normalisation sample  $B^0 \rightarrow K^{*0}J/\psi$  to obtain the values for  $F_S$  and  $A_S$  to be used in the simultaneous fit to the invariant mass and the angular distributions. In the LHCb study, the set of variables,  $A_{FB}$ ,  $F_L$ ,  $S_3$  and  $A_9$ , is extracted by a fit to the  $K\pi\mu\mu$  invariant mass,  $\cos\theta_\ell$ ,  $\cos\theta_K$  and  $\phi$  distributions. The angular signal distributions need to be corrected for angular detector efficiencies due to trigger, event reconstruction, detector effects and selection cuts. For this reason, the angular signal distributions are weighted by efficiency correction factors obtained from the Monte Carlo.

The differential branching fraction of the signal decay  $B^0 \rightarrow K^{*0}\mu^+\mu^-$ , in each  $q^2$  bin, is estimated by normalising the signal yield,  $N_{\text{sig}}$ , to the total event yield of the  $B^0 \rightarrow K^{*0}J/\psi$  control sample,  $N_{K^{*0}J/\psi}$ , and correcting for the relative efficiency,  $\epsilon_{K^{*0}J/\psi}/\epsilon_{K^{*0}\mu^+\mu^-}$ ,

<sup>1</sup>They include  $B_s \rightarrow \phi(1020)\mu\mu$ ,  $\Lambda_b \rightarrow \Lambda^*(1520)\mu\mu$ ,  $B_s \rightarrow K^{*0}\mu\mu$ ,  $B^0 \rightarrow J/\psi K^{*0}$ ,  $B^0 \rightarrow \psi(2S)K^{*0}$ , and  $B^+ \rightarrow K^+\mu\mu$ .

$$\frac{d\mathcal{B}}{dq^2} = \frac{1}{q_{\max}^2 - q_{\min}^2} \frac{N_{\text{sig}}}{N_{B^0 \rightarrow K^*0 J/\psi}} \frac{\mathcal{E}_{B^0 \rightarrow K^*0 J/\psi}}{\mathcal{E}_{K^*0 \mu^+ \mu^-}} \times \mathcal{B}(B^0 \rightarrow K^*0 J/\psi) \times \mathcal{B}(J/\psi \rightarrow \mu^+ \mu^-). \quad (2.1)$$

The number of signal candidates in each of the  $q^2$  bins is estimated by performing an extended unbinned maximum likelihood fit to the  $K\pi\mu\mu$  invariant mass distribution.

### 3. Results and conclusions

The results of the analyses performed by ATLAS, CMS and LHCb [10, 11, 12] are given in Figs. 1 and Fig. 2 reporting the measurements of  $F_L$ ,  $A_{FB}$ , and  $d\mathcal{B}/dq^2$  as a function of  $q^2$ .

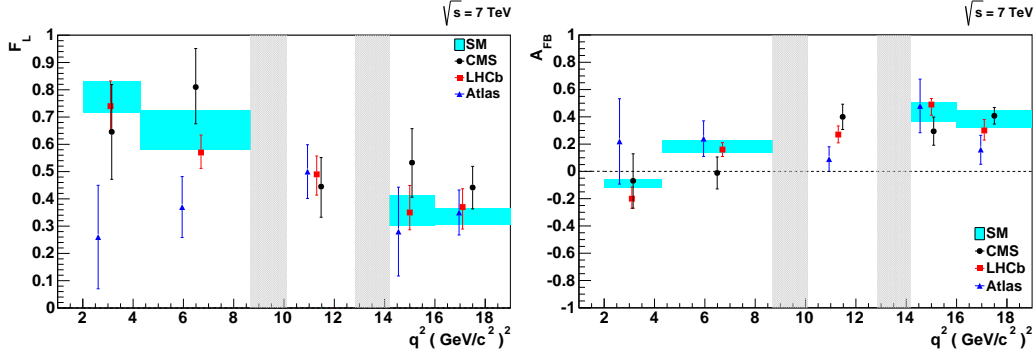


**Figure 1:** Results of the measurement of  $F_L$  (left) and  $A_{FB}$  (right) versus the di-muon  $q^2$ . The error bars correspond to the total uncertainty. The gray shaded regions correspond to the  $J/\psi$  and  $\psi'$  resonances. The Standard Model prediction [1] is given by the cyan (light) band after rate-averaging across the  $q^2$  bins to allow direct comparison to the data points.

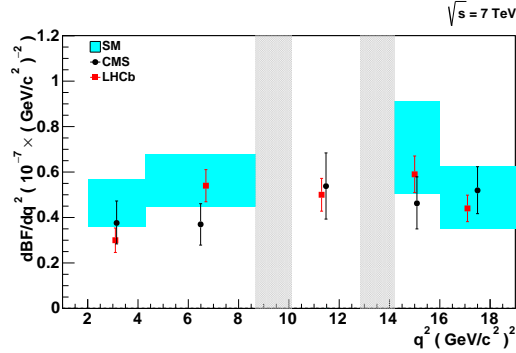


**Figure 2:** Results of the measurement of  $d\mathcal{B}/dq^2$  versus the di-muon  $q^2$ . The error bars correspond to the total uncertainty. The gray shaded regions correspond to the  $J/\psi$  and  $\psi'$  resonances. The Standard Model prediction [1] is given by the cyan (light) band after rate-averaging across the  $q^2$  bins to allow direct comparison to the data points.

LHCb errors are smaller, while the ATLAS and CMS errors are comparable. All measurements are compatible with the Standard Model expectations, but for the  $F_L$  observable at low  $q^2$  measured by ATLAS, which is slightly off by  $\sim 2\sigma$ . The three experiments performed also the measurements in the special  $q^2$  bin  $1 < q^2 < 6$  ( $\text{GeV}/c^2$ )<sup>2</sup>, which is the region where the theoretical predictions are the most accurate. The results are reported in Table 1. All measurements are compatible with each other. The small tension in the ATLAS measurement of  $F_L$  is also present here. In

**Table 1:** Measurements from ATLAS, CMS and LHCb of the fraction of longitudinal polarisation of the  $K^*$ ,  $F_L$ , the forward-backward asymmetry of the muons,  $A_{FB}$ , and the branching fraction for  $B^0 \rightarrow K^{*0} \mu^+ \mu^-$  in the region  $1 < q^2 < 6$  ( $\text{GeV}/c^2$ )<sup>2</sup>. The first uncertainty is statistical and the second is systematic.

Experiment	$F_L$	$A_{FB}$	$d\mathcal{B}/dq^2$ ( $10^{-8} \times c^4/\text{GeV}^2$ )
ATLAS	$0.18 \pm 0.15 \pm 0.03$	$0.07 \pm 0.20 \pm 0.07$	—
CMS	$0.68 \pm 0.10 \pm 0.02$	$-0.07 \pm 0.12 \pm 0.01$	$4.4 \pm 0.6 \pm 0.7$
LHCb	$0.65^{+0.08}_{-0.07} \pm 0.03$	$-0.17 \pm 0.06 \pm 0.04$	$3.4 \pm 0.3^{+0.4}_{-0.5}$

addition, the LHCb experiment performed the first measurement of the zero-crossing point to be  $4.9 \pm 0.9 \text{ GeV}^2/c^4$ , which is in good agreement with the SM predictions.

All three experiments are in the process of analysing the data collected during the 2012 run, where LHCb collected  $\sim 2 \text{ fb}^{-1}$ , while ATLAS and CMS collected  $\sim 22 \text{ fb}^{-1}$ . ATLAS and CMS foresee to extend the fit to include also the  $\phi$  angle, just like LHCb did for the analysis of 2011 data. Moreover, at LHCb it might be possible to perform a full angular analysis and measure all observables of the decay rate in Eq. 1.1.

## References

- [1] Christoph Bobeth, Gudrun Hiller, and Danny van Dyk. *Phys. Rev. D*, 87:034016, 2013.
- [2] Wolfgang Altmannshofer et al. *JHEP*, 0901:019, 2009.
- [3] Damir Becirevic and Elia Schneider. *Nucl.Phys.*, B854:321–339, 2012.
- [4] Joaquim Matias, Federico Mescia, Marc Ramon, and Javier Virto. *JHEP*, 1204:104, 2012.
- [5] Bernard Aubert et al. *Phys. Rev.*, D79:031102, 2009.
- [6] J.-T. Wei et al. *Phys.Rev.Lett.*, 103:171801, 2009.
- [7] T. Aaltonen et al. *Phys.Rev.Lett.*, 107:201802, 2011.
- [8] T. Aaltonen et al. *Phys.Rev.Lett.*, 108:081807, 2012.
- [9] Joaquim Matias. *Phys.Rev.*, D86:094024, 2012.
- [10] ATLAS collaboration. ATLAS-CONF 2013-038, 2013.
- [11] CMS collaboration. CMS PAS BPH-11-009, 2013.
- [12] LHCb collaboration. arXiv:1304.6325 [hep-ex], 2013.
- [13] ATLAS Collaboration. *JINST*, 3:S08003, 2008.
- [14] S. Chatrchyan et al. *JINST*, 3:S08004, 2008.
- [15] Jr. Alves, A. Augusto et al. *JINST*, 3:S08005, 2008.